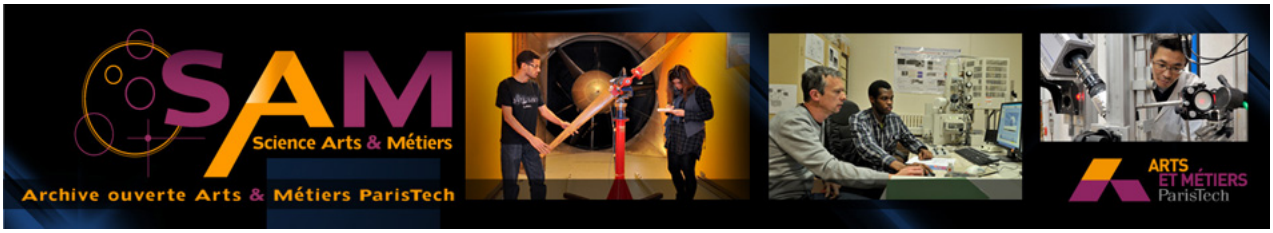

Multiscale Roughness Analysis in Injection-Molding Process

Maxence Bigerelle,[1] Adrien Van Gorp,[1,2,3] Alain Iost[3]
[1] *Laboratoire Roberval, UMR 6253, UTC/CNRS, Centre de Recherches de Royallieu, BP20529, 60205 Compiègne, France*

[2] *Visteon Systèmes Intérieurs, Technical Center Harnes, Rue Léon Duhamel, BP 87, 62440 Harnes, France*

[3] *Equipe Caractérisation et Propriétés de la Périsurface, LMPGM, UMR CNRS 8517 Arts et Métiers ParisTech, 8 Boulevard Louis XIV, 59046 LILLE Cedex, France*

The roughness of polymer surfaces is often investigated to guarantee both the surface integrity and the surface functionality. One of the major problems in roughness measurement analyses consists in determining both the evaluation length and the reference line (i.e., the degree of the polynomial equation) from which roughness parameters are computed. This article outlines an original generic method based on the generalized analysis of variance and experimental design methodology for estimating the most relevant roughness parameter *p*, the most pertinent scale, *s*, and finally, the degree of the polynomial fitting, *d*. This methodology is then applied to characterize the influence of four process parameters on the final roughness of poly(polypropylene) samples obtained by injection molding. This method allows us to determine the most efficient triplet (*p, s, d*) that best discriminates the effect of a process parameter *q*. It is shown that different (*p, s, d*) values are affected to each process parameter giving finally the scale on which each process parameter modifies the roughness of a polymeric surface obtained by injection molding. POLYM. ENG. SCI., 48:1725–1736, 2008. © 2008 Society of Plastics Engineers

INTRODUCTION

In microinjection molding, the quality and topography of the machined surface have a significant impact on the replication capabilities (filling) [1]. Particularly, the surface topography of polymer influences adhesion and is correlated to asperities' density [2]. The morphology of the grooves (depth and spacing) enhances the effective adhesion between two immiscible polymers with increasing toughness as groove spacing decreases and groove depth increases [3]. For polymer-based materials, the measurement of roughness (e.g., the R_a) may also provide a new method for evaluating the biodegradation [4]. A rough surface can be formed by UV-degradation that leads to gloss loss [5]. However, the relevant scale from which roughness is evaluated is still in controversy. For example, the cell interaction with biomaterial polymeric surfaces is very sensitive to the roughness variations that occur at the nanometer length by changing the crystallinity [6]. This scale effect was met in injection molding: the ejection forces decrease as the mold surface roughness decreases [7], but these results are in disagreement with Dearnley's results that find that coated or uncoated polished surfaces produce lower friction forces during ejection compared to coated or uncoated spark-eroded surfaces [8]. In this work, it will be proven that this inversion of correlation with different molding-process parameters can be related to the evaluation length used to calculate the roughness parameters. As a consequence, a multiscale approach must be performed before finding a correlation between physical properties of the surface such as wetability [9], surfacic mechanical properties [10], optical properties [11], quality of machining [12], stick slip [13], and the surface roughness.

Two major problems in analyzing the roughness parameters consist in determining both the evaluation length and the reference line (i.e., the degree d of the polynomial fitting) from which roughness parameters are computed [14]. Another difficulty is to select the parameter, which characterizes at best the surface roughness [15]. These two observations involve that the value of a roughness parameter, denoted p_i, will both depend on the degree d of the reference line and the evaluation length L of the

profile on which it will be estimated. This parameter will be noted p_i (d, L), and the main feature is to select (d, L).

In this article, to avoid an intuitive selection of (d, L), a quantitative measure of the pair (d, L) relevance will be developed. This choice cannot be dissociated from physical phenomena that interact with the surfaces at a given scale. As a consequence, the length on which the profile will be measured must maximize a mathematical function including interaction between physical phenomena and the surface. Physical interactions with a surface can be briefly classified in two categories: the physical phenomenon interacts with the surface (electromagnetic waves on rough surfaces such as brightness, fluid interaction defined by the Reynolds number, etc.) or surface roughness is created by a physical process (such as surface coating, casting process, and polishing). Between these two extreme cases, the physical system can interact differently with the roughness of the surface and also modify it (wear on roughness surfaces). We postulate that if the amplitude of a physical phenomenon that interacts with the surface varies and depends on the roughness, then there is a mathematical measure that will be optimal at a given evaluation length. More precisely, a statistical threshold is required to reject interaction between surface morphology and the physical response at a fixed scale. This function, noted $\Theta(\psi_j, p_i(d,L))$, characterizes at best the interaction between the phenomenon ψ_j and the surface by quantifying the effects of the selection of the roughness parameter p_i, the scale L at which it will be measured and finally the degree d of the reference line. In this work, we focus on the k discrete values of the physical phenomena ψ_j noted $\psi_{j,k}$. To determine the influence of the rough substrate surfaces on adhesion, Brown and Siegman [16] used a fractal analysis based on a patchwork method at a given scale L. They measured the relative area $A(L)$ that has been covered in the tiling and constructed a $\Theta(\psi, A(L))$ function, where ψ is adhesive strength and Θ the measure of correlation between ψ and $A(L)$. The maximal value $[\Theta(\psi, A(L_{\min})), \Theta(\psi, A(L_{\max}))]$ gives the scale of adhesion. Scott et al. [17] analyzed dental microwear texture of extinct primate. They used four parameters p_i: heterogeneity, textural fill volume, complexity, and anisotropy are used as Θ, a Kruskal–Wallis statistics. This analysis illustrates how these parameters distinguish extant primates with different diets [18]. Narayan et al. [19] compare conventional surface metrology and area-scale fractal parameters to differentiate the surface topography of pharmaceutical excipient compacts and used as Θ, a F statistic.

This article is organized as follows. In Molding process and surface measurements, an experimental design related to an injection-molding process is used to quantify the influence of the process parameters on sample roughness. In Roughness measurements, the mathematical method used to calculate the multiscale reference line is introduced, followed by the multiscale roughness parameter evaluation method (The multiscale roughness parameters). In The mathematical formalism, the mathematical definition of the multiscale discrimination function $\Theta(\psi_j, p_i(d,L))$ is introduced by using generalized analysis of variance. Finally, we shall expose in Results and discussion, the influence of the process parameters on the surface roughness, taking into account the best roughness parameter, the most appropriate degree of polynomial regression and the most pertinent roughness evaluation length. In Appendix, conventional method and Fourier analyses are proceeded to compare results with the proposing method.

MOLDING PROCESS AND SURFACE MEASUREMENTS

Purpose

In this section, the influence of process parameters on the aspect of specimens obtained by plastic injection is studied. Under particular injection conditions, some manufacturing defects like gloss differences can be observed and linked with roughness variations.

Experimetal Design

Plates are produced by injection molding. The surface is grained, and the purpose was to identify the influence of injection parameters on the roughness, in particular, by considering the optimal scale at which the study has to be performed. The injected material was a 20% talc-filled polypropylene (CMV205 supplied by EXXON Mobil®). Thanks to a two-level factorial experimental design, the influence of four process parameters is studied ($2^4 = 16$ configurations). The retained parameters are injection temperature ($T = 180$°C and 250°C), injection velocity ($V =$ 5 and 140 mm/s) corresponding to the screw (Ø 50 mm) displacement, dosing pressure (cp = 5 and 15 bars), and time between the end of injection and ejection of the plate (tr = 18 and 55 s). To ensure stabilized process conditions, for each configuration, 10 plates have been injected and only the last one was analyzed.

Roughness Measurements

To quantify the surfaces' anisotropy related to the molding process, for each configuration, 30 roughness profiles are recorded both in the injection direction and perpendicular to this one. Each of them was recorded with a sampling length of 0.1 μm, a scanning length of 8 mm, and a scanning speed of 100 μm/s by a 3D tactile surface profilometer KLA TENCOR® P10 with a 1-μm stylus radius and a 5 mg load. Its resolution is 10 nm, 50 nm, and 1 μm, respectively, on the z, x, and y axis. Each profile was fitted by a third degree polynomial function (least squares method) to remove the form, keeping only waves and roughness.

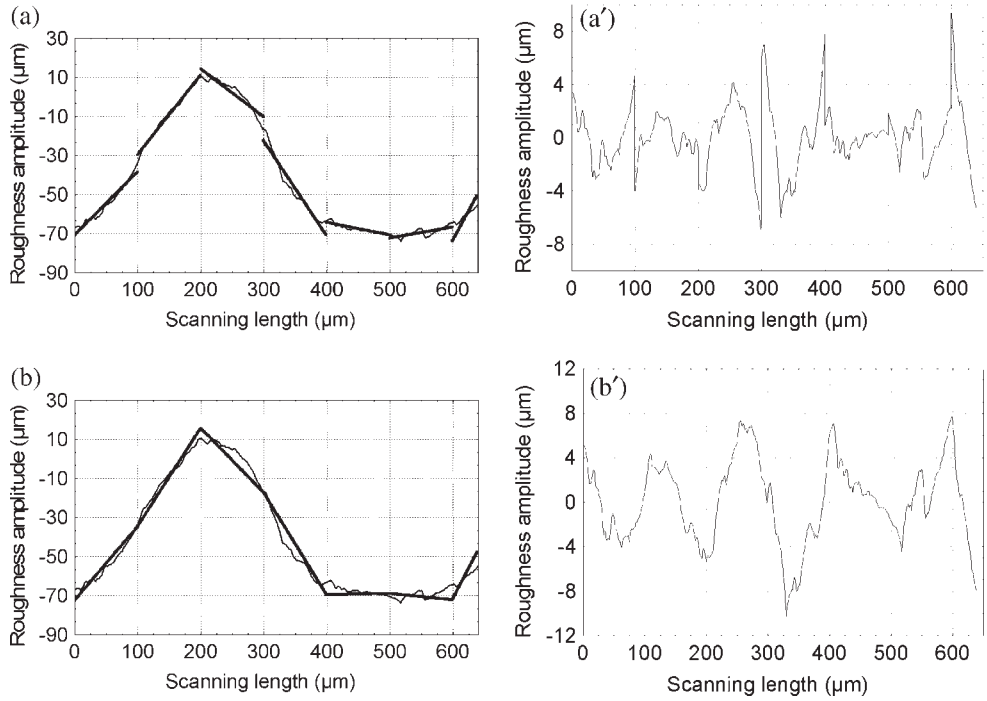

FIG. 1. The discontinuous regression line (a) continuous one (b) applied on to polymeric surfaces recorded with a tactile profilometer and the final profiles from which roughness parameters will be estimated (a′) and (b′).

LOCAL FITTING

Each experimental profile is split into equal parts considered as the evaluation length. To delete "the shape" greater than the evaluation length, each profile part has been rectified by polynomial least square fitting using discontinuous or continuous regression.

Discontinuous Regression

Polynomial least square fittings are calculated on each part of the profile, without taking account of the foreign parts. Figure 1a presents the linear regression lines corresponding to an evaluation length of 100 μm, in which, at each window boundary, some discontinuities of the global fitted curves can be observed as they appear on the final profile from which the roughness parameters will be estimated (Fig. 1b). Indeed, if a reconstruction of the profile is processed after form removal, the discontinuities, which creates an artificial roughness—independent of the process itself—will be preserved on the rectified profile,

Continuous Regression

To remove the local forms, without including the numerical artefacts mentioned earlier, the regression parameters are computed on a given window by imposing a $C^{\text{d-1}}$ continuity between adjacent polynomials defined on the two neighbor's windows. As a consequence, the form profile is a B-spline function [20] described by the parametric representation $\mathbf{B}(t) = \begin{vmatrix} X(t) \\ Y(t) \end{vmatrix}$, which minimizes the quadratic distance with regard to the profile. This B-spline is defined by a list of control points $\{\mathbf{P_0},\mathbf{P_1},\ldots,\mathbf{P}_K\}$, whose number K corresponds to the number of windows along the scanning length and the associated knot sequence $\{u_0,u_1,\ldots,u_K\}$. More precisely, a B-spline can be written as follows: $\mathbf{B}_{d,K}(t) = \sum_{i=0}^{K} \mathbf{P_i} \cdot N_{i,d}(t)$, where $\mathbf{P_i} = \begin{vmatrix} X_i \\ Y_i \end{vmatrix}$ are the control points and $N_{i,d}$ is the polynomial function with degree d defined by the recursive scheme [20]:

$$N_{i,n}(t) = \frac{t-u_{i-1}}{u_{i+n-1}-u_{i-1}} N_{i,n-1}(t) + \frac{u_{i+n}-t}{u_{i+n}-u_i} N_{i+1,n-1}(t);$$
$$\text{with} \quad N_{i,0}(t) = \begin{cases} 1 & \text{if } t \in]u_{i-1},u_i] \\ 0 & \text{else} \end{cases} \tag{1}$$

For simplicity, we select $X(t) = t$ and the fitting problem becomes a minimization of the quadratic distance

$$\sum_{i=0}^{L} \|y_i - Y(x_i)\|^2 \tag{2}$$

with $\begin{vmatrix} x_i \\ y_i \end{vmatrix}$ the coordinates of the L points of the profile, that corresponds to:

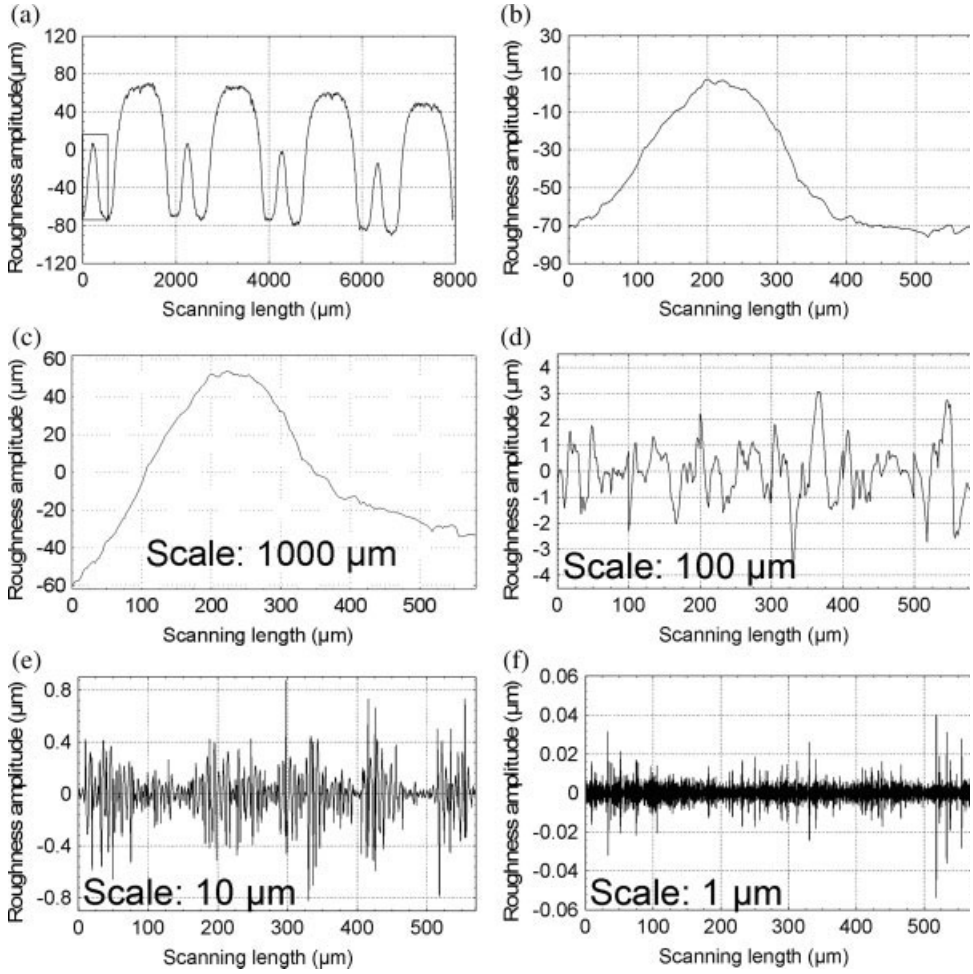

FIG. 2. Multiscale profile reconstructions (rectified with a second degree polynomial fitting) corresponding to evaluation lengths L: (a) the whole profile $L = 7950$ μm, (b) zoom of profile included in the box of (a), (c) $L = 1000$ μm, (d) $L = 100$ μm, (e) $L = 10$ μm, and (f) $L = 1$ μm.

$$\sum_{i=0}^{L}\left[y_i - \sum_{j=0}^{K} Y_j \cdot N_{j,n}(x_i)\right] N_{Q,n}(x_i) = 0 \quad \forall Q \in \{0, ..., K\} \tag{3}$$

or

$$\overrightarrow{\mathbf{Y}} = \overline{\overline{\mathbf{M}}}.\overrightarrow{\mathbf{P}} = \begin{vmatrix} \sum_{i=0}^{L} y_i \cdot N_{0,n}(x_i) \\ \vdots \\ \sum_{i=0}^{L} y_i \cdot N_{Q,n}(x_i) \\ \vdots \\ \sum_{i=0}^{L} y_i \cdot N_{K,n}(x_i) \end{vmatrix} \quad \text{with} \quad \overrightarrow{\mathbf{P}} = \begin{vmatrix} Y_0 \\ \vdots \\ Y_Q \\ \vdots \\ Y_K \end{vmatrix} \tag{4}$$

with:

$$\overline{\overline{\mathbf{M}}} = \left(m_{j,k}\right) \quad \text{and} \quad m_{j,k} = \sum_{i=0}^{p} N_{j,n}(x_i) \cdot N_{k,n}(x_i) \tag{5}$$

Using *Eqs. 1–5*, vector $\overrightarrow{\mathbf{P}} = \left(\overline{\overline{\mathbf{M}}}\right)^{-1} \cdot \overrightarrow{\mathbf{Y}}$ is obtained. After the B-spline curve calculation, the profile is rectified by subtracting the B-spline. Figure 1b presents the linear regression lines corresponding to an evaluation length of 100 μm, and Fig. 1b′ presents the final profile from which roughness parameters will be estimated. If so, the equation defined by the B-spline would present a more realistic representation of the profile form without including artificial roughness.

Figure 2 presents the reconstructions of the same profile rectified by a second-degree polynomial regression fitting corresponding to four different evaluation lengths from 1 to 1000 μm. For a given evaluation length, the reconstructed profiles show that the rectification corresponds to a set of high pass filters, which reveal the microroughness. This analysis is in agreement with the scanning electron microscopy observations (see Fig. 3): at the macroscopic level, shapes represent forms given by the periodic motif and at the microscopic one, shapes are given by the grain of the polymer's microstructure.

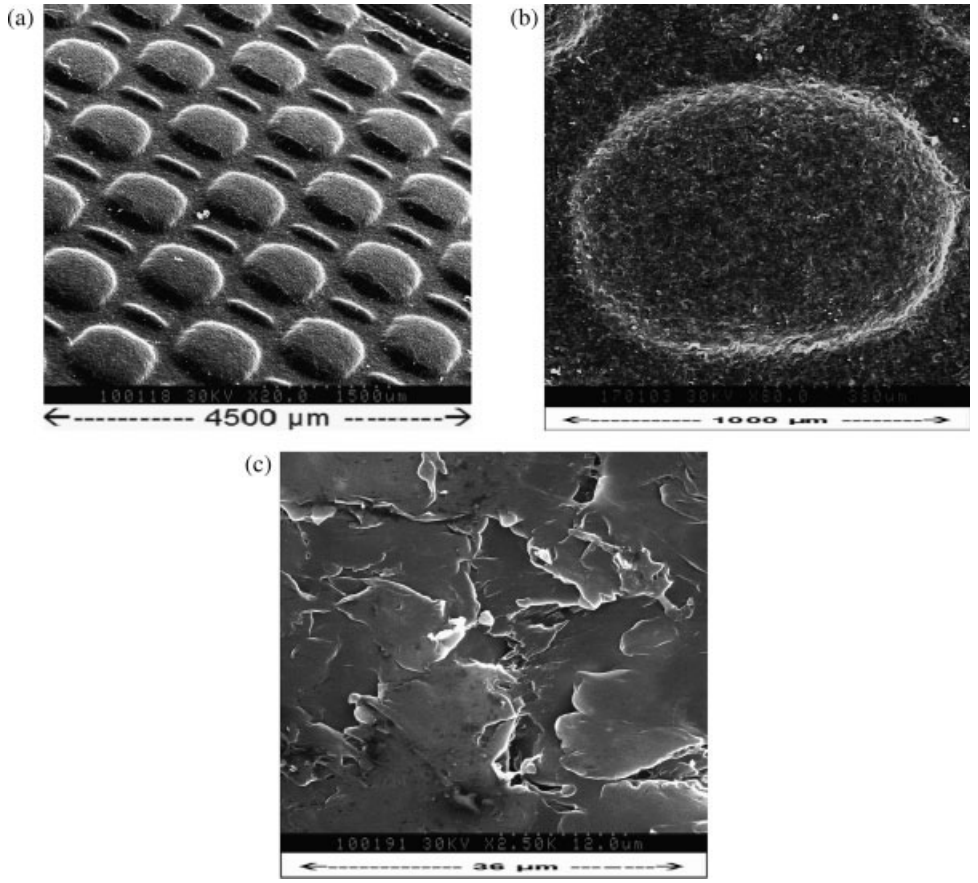

FIG. 3. SEM images of a plate surface under three magnifications (×20, ×80, ×2500).

THE MULTISCALE ROUGHNESS PARAMETERS

From all d degree rectified profiles described in Local fitting, roughness parameters are calculated on all sub parts of fixed evaluation length L. Then, the average value of each roughness parameter q, noted $q_i(d,L)$, is calculated by averaging on all equal parts of the profile. Thereafter, this step is reproduced for different evaluation lengths and different polynomial fitting degrees. For this investigation, the roughness profile is supposed to be ergodic, that is, roughness is homogeneous along the whole evaluation length of the profile. In this case, all multiscale measures are not spatially located, and therefore our multiscale approach is quite different from the wavelet analysis [21–23].

For the two-injection directions, Fig. 4 represents the Ra parameter mean value (mean calculated from all the 30 × 8 profiles) versus the evaluation length and the injection temperature when the reference line is calculated by a second order regression. When applied to discontinuous linear-regression fitting, this representation can be found in bibliography [24, 25]. A slightly higher Ra can be observed for higher injection temperature at the evaluation length of 10–100 μm. However, this difference is more obvious in the flow direction. At this stage, it is not possible to conclude if this difference is significant and if the most accurate roughness parameter and the most relevant degree of reference line have been selected. This point will be discussed in the following paragraphs. It must be emphasized that the log–log plot presents a linear tendency for small evaluation length values that can be linked with the fractal dimension of the profile, Δ. For example, taking $q_i = Rt$, Tricot [26] shows that the slope H of the log–log plot estimates the fractal dimension of the profile ($\Delta = 2H$) at small evaluation lengths. However, this linearity fails in our graphs. Consequently, limiting the multiscale analysis only to the fractal dimension reduces the multiscale profile information. Let us now analyze the aspect of these curves. First, up to a 2 μm length, the graphic relation between Ra and L is curved downward, because the profilometer tip radius (1 μm) smoothes the surface and decreases the roughness amplitude [27]. At a 2 μm scale, the roughness amplitude reaches a first threshold (linear stage) and then a second one (a plate in the roughness as a consequence of the repetition of the grained structure (i.e., periodical motifs).

THE MATHEMATICAL FORMALISM

To solve our problem, we use the well-known ANOVA analysis of variance. It is an implementation of the

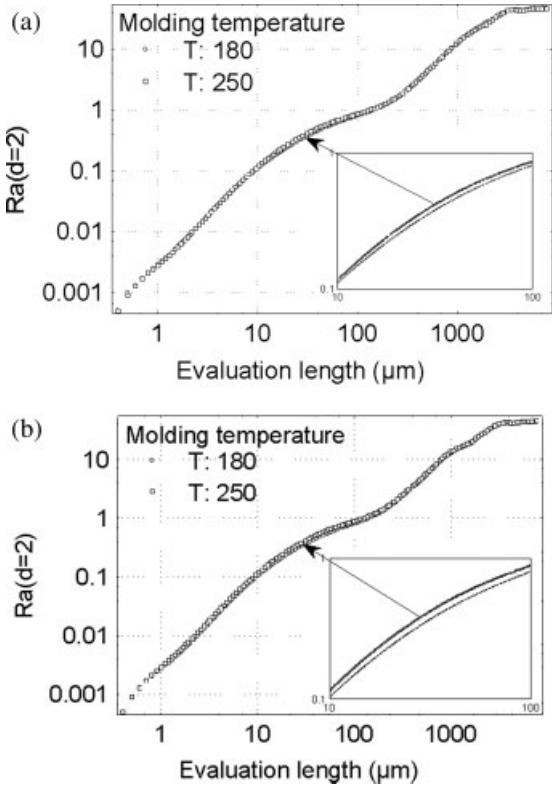

FIG. 4. Evolution of the mean R_a parameter (reference line is a two degree polynomial equation) versus the scanning length for two injection temperatures (180 and 250°C). (a) Roughness measured perpendicular to the flow and (b) roughness measured in the flow direction.

general linear model [28, 29], which is a powerful technique to test the relevance of our approach [30]. In our case, the ANOVA model can be stated as follows:

$$q_i(d,L,k_1,k_2,\ldots,k_p,n) = \alpha_0 + \sum_{j=1}^{p} \alpha_{j,k_j}(i,d,L) + \sum_{j=1}^{p}\sum_{l=j+1}^{p} \beta_{j,k_j,l,k_l}(i,d,L) + \xi_{k_1,k_2,\ldots,k_p,n}(i,d,L) \quad (6)$$

where $q_i(d,L,k_1,k_2,\ldots,k_p,n)$ is the value of the roughness parameter q_i of the nth profile when the p process parameters are taken at levels $k_1,k_2,\ldots,k_p$, for rectified profile with a d degree polynomial on an evaluation length L. $\alpha_{j,k_j}(i,d,L)$ is the influence of the roughness value of the jth process parameter at level k_j, and $\beta_{j,k_j,l,k_l}(i,d,L)$ is the influence of the interaction value between both process parameters k_j and k_l. $\xi_{k_1,k_2,\cdots,k_p,n}(i,d,L)$ is a Gaussian noise with null mean value and standard deviation σ.

The program will first compute the within-cell variance/covariance matrix of process variables (and covariates see below). The design matrix of main effects and interactions is first ortho-normalized and then used to compute the sums of square hypotheses (from the cell means) and sums of square errors (from the within-cell variance/covariance matrix). The output of the analysis includes statistical information about the levels of the variable process under analysis, that is, the degrees of freedom, sum of squares, and the mean square for the model and random error. "Root MSE" is the square root of the mean square for error. Our pertinence measure will be the Fisher variate $F[q_i(d,L,k_j)]$ value, which is the ratio produced by dividing the mean square for the model at configuration j [or (j,l) for interaction] by the mean square for error (and $F[q_i(d,L,k_j,k_{j'})]$ for interaction). If the model does not really affect the expected value of the response, then the two mean square should be about the same ($F[q_i(d,L,k_j)] \cong 1$); on the contrary, a Model mean square much larger than the error mean square ($F[q_i(d,L,k_j)] >> 1$) indicates that the model does in fact affect the response. To reject the fact that a process parameter does not modify the surface roughness parameters, the relation $F[q_i(d,L,k_j)] > F_0(\theta)$ must hold, where $F_0(\theta)$ is a Fisher variable at a confidence interval θ. The higher the θ, the lower the probability to affirm wrongly that a process parameter influences a roughness parameter. By varying the length value L for the roughness parameter q_i and the polynomial degree d, the scale influence $F[q_i(d_j,L,k_m)]$ is plotted versus the evaluation length L. Then, taking the maximal value of these curves, the multiscale discrimination function is constructed:

$$\Theta(k_m) = \left(q_{\text{opt}}, d_{\text{opt}}, L_{\text{opt}} \middle| F_{\text{opt}} = \max_{i,d,L}(F[q_i(d,L,k_m)])\right) = \left(F_{\text{opt}}, q_{\text{opt}}, d_{\text{opt}}, L_{\text{opt}}\right) \quad (7)$$

For the considered process parameter k_m, *Eq. 7* gives the roughness parameter q_{opt}, the degree d_{opt} and the length L_{opt} on which the process is the most influent on the surface roughness. In the cases of interactions between two process parameters (k_m,k_n), *Eq. 7* becomes

$$\Theta(k_m,k_n) = \left(q_{\text{opt}}, d_{\text{opt}}, L_{\text{opt}} \middle| F_{\text{opt}} = \max_{i,d,L}(F[q_i(d,L,k_m,k_n)])\right) = \left(F_{\text{opt}}, q_{\text{opt}}, d_{\text{opt}}, L_{\text{opt}}\right) \quad (8)$$

RESULTS AND DISCUSSION

In this study, we focus on three main amplitude roughness parameters (R_a, R_q, and R_t). The polynomial degree varies from 0 to 2 and the evaluation length from 10 times the sampling length to the total recording of the process.

General Analyses

Rather than a general description and without lack of generality, we considered only the injection temperature effect on the roughness to analyze the multiscale curves of relevance. $F[R_a(d,L,t)]$, $F[R_t(d,L,t)]$, and $F[R_q(d,L,t)]$ are computed for the two scanning directions (perpendicu-

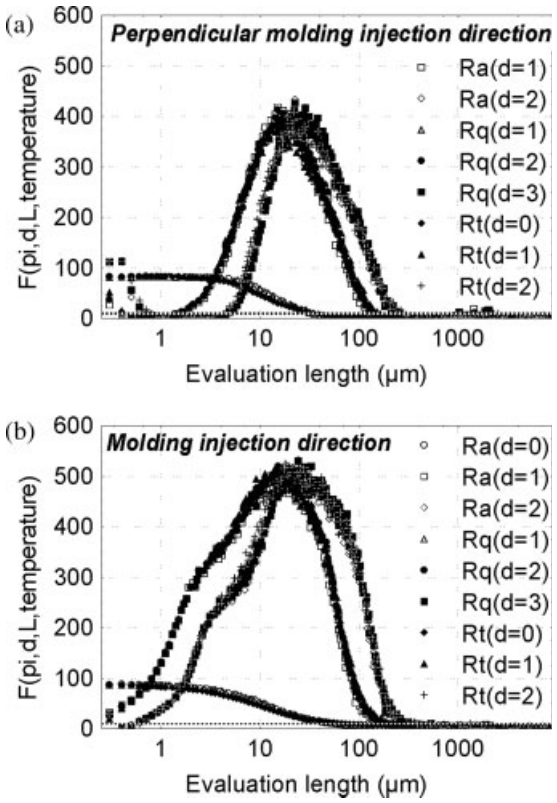

FIG. 5. Evolution of the scale pertinence functions $F\left[q_i(d_j, L, k_m)\right]$ versus the evaluation length L due to the effect of the temperature injection $k_m = T$ for roughness parameters $q_i = \{R_a, R_t, R_q\}$ and polynomial degrees $d_j = \{0, 1, 2\}$: (a) roughness measured perpendicular to the flow and (b) roughness measured in the flow direction.

lar and parallel to the flow) for 0, 1, and 2 polynomials degrees.

From Fig. 5, some general remarks can be stated:

No significant difference appears between the discrimination function calculated from the R_a, R_t, and R_q amplitude parameters. All of them present the same discrimination value on a similar evaluation length and for all degrees. All the curves related to the others process parameters (not shown) present the same trend. As these roughness parameters get the same power of discrimination, any of them possesses individually more information to characterize the process and they are thus redundant. This result may be surprising but must be investigated further. First time, we can expect that R_t is the least robust, and then its variance is greater than that of the other parameters. This assertion is right when R_t is evaluated on the whole scanning length as a consequence to it high extreme values sensitivity. However, in the scale of pertinence, R_t is highly averaged leading to decreasing extreme variations. Finally, it has the same accuracy as R_a and R_q. This entails that the same relevance is obtained by taking a larger scan length than the pertinent one and averaging values of the amplitude parameters. In fact, we extended the definition of the well-known parameter called "Average Maximum Profile Peak Height," R_{pm}, defined in the ASME B46.1-2002 norm, which is the mean roughness on fixed part of profiles. Briefly summarized, the degree and the length, where these parameters are computed, are of higher interest than the choice between these three parameters.

By our method, the highest value of the discriminant function is used to characterize the most relevant scale. The scale given is not punctual (as obtained by the wavelet), but rather a scale interval of pertinence $\left[L_{\inf}, L_{\sup}\right]$ defined as follows:

$$\forall L \in [L_{\inf}, L_{\sup}], \quad L_{\text{opt}} \in [L_{\inf}, L_{\sup}],$$
$$F[q_i(d, L_{\inf}, k_j)] = F[q_i(d, L_{\sup}, k_j)] = F_0(\theta) \Vert$$
$$F[q_i(d, L, k_j)] > F_0(\theta) \qquad (9)$$

Applied on $R_a(d = 1, L, t)$, we get $L_{\min} = 3$ μm, $L_{\text{opt}} = 15$ μm, and $L_{\max} = 100$ μm meaning that the effect of temperature can be detected by R_a on an [3 μm, 100 μm] evaluation length, with maximal pertinence at scale $L = 15$ μm. An important remark has to be pointed out: the optimal value is not centered in the interval, meaning that the high pertinence is located in a small scale interval rather than in a higher one. This skewness can be explained by two mechanisms. First, length $L_{\inf}$ corresponds to the beginning of the relevant scale range. This can be explained by the fact that the number of sampling points of the profile is low, and as a consequence, error on the estimation of local polynomial coefficients increases. This increasing error raises the variation of the considered roughness parameter and finally decreases the F value. Second, the form of the roughness due to the process itself is retrieved at this scale. When evaluation length increases progressively in $\left[L_{\inf}, L_{opt}\right]$, the whole form of the roughness due to the process is integrated. Above L_{opt}, forms of larger scales (macro roughness), which are not due to the process parameters, are included in the signal analysis and fatally decrease relevance.

For $d = 0$, the curves present a particular shape, different from curves of higher degree (Fig. 6). The zero degree does not retrieve the nonpertinent macroscopic forms. Indeed, only at large scales, the roughness due to the process itself is highly perturbed by the component of the macroroughness and therefore this macroroughness can be neglected only at very small scales.

Increasing the polynomial degree of regression shifts the bell-shape curves to the right, i.e., to higher evaluation lengths. By increasing the degree on a fixed scale between $\left[L_{\inf}, L_{opt}\right]$, rectifications fatally risks to suppress the roughness information created by the process itself. On the contrary, having a high level of F on higher scale, the degree of polynomial must be increased to suppress the form that is not due to the process itself.

Multiscale Roughness of the Molding Process

For the most pertinent roughness parameter, the degree of polynomial regression and evaluation length are repre-

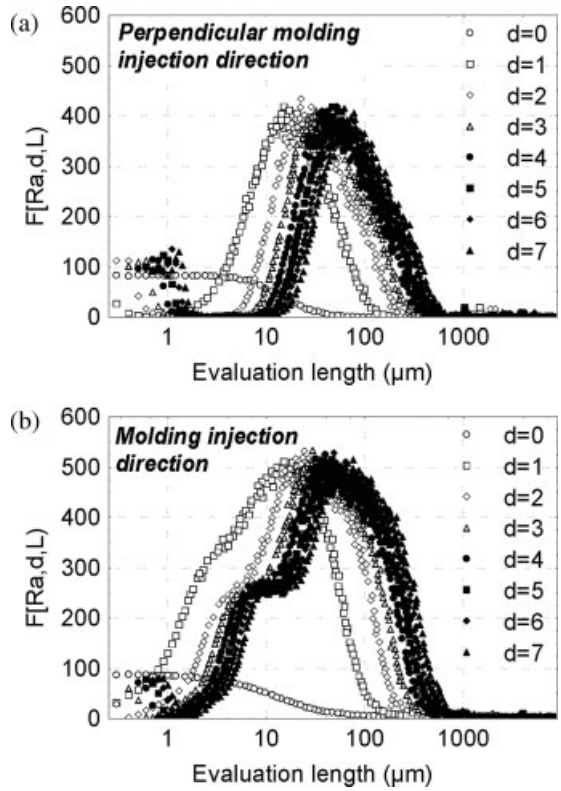

FIG. 6. Evolution of the scale pertinence functions $F\left[R_a(d_j, L, T)\right]$ versus evaluation length L calculated from a reference line of $d_j = \{0, 1, \ldots, 7\}$ degree polynomial equation: (a) roughness measured perpendicular to the flow and (b) roughness measured in the flow direction.

sented in Table 1 for all the process parameters and their associated interactions.

Influence of the Molding Temperature. R_a measured at the scale 23 μm and a second polynomial degree is the best discriminating parameter whatever the molding injection direction ($\Theta(T)_{\mathrm{ID}} = (532, R_a, 2, 24)$ and $\Theta(T)_{\mathrm{PID}} = (434, R_a, 2, 22)$). The R_a increases with temperature from 0.275 μm ($T = 180^{\circ}$C) to 0.305 μm ($T = 250^{\circ}$C) in the perpendicular injection direction (PID) and from 0.285 to 0.332 μm in the injection direction (ID). As no difference occurs on the degree and scale for both directions, it can be stated that temperature effect on roughness is related to the same mechanism. This R_a increase can be explained by a decrease in viscosity associated with an increase in temperature that enlarges the contact area with the metallic die and promotes the roughness replication at small scale (around 23 μm). This analysis was confirmed, because the melting temperature improves the polymer flow as a consequence to a reduction of material viscosity and shear stress [31]. Besides, high melting and mold temperatures facilitate the filling of microcavities [32].

Influence of the Molding Injection Velocity. Analysis leads to $\Theta(V)_{\mathrm{ID}} = (562, R_a, 2, 85)$ and $\Theta(T)_{\mathrm{PID}} = (560, R_a, 2, 74)$ (see Fig. 7). The velocity effect is concentrated at a 80-μm scale, larger than the temperature effect. R_a increases with injection speed from 0.275 μm ($v = 5$ mm/s) to 0.305 μm ($v = 140$ mm/s) in the PID and from 0.285 to 0.332 μm in ID. When v increases, the mold is filled faster, and then the polymer stays longer at high temperature than in slow injection speed. Fatally, the viscosity will be lower, involving a better roughness transfer from the mold to the plate. For the PID direction, a bimodal F-curve can be observed, meaning that the injection velocity modifies the polymer roughness at two different scales. This bimodal scale does not appear in the injection direction. The interpretation of this result is under investigation. In general, high injection rates lead to high shear rates that could increase the friction between the mold surface and the melt flow in the cavities, and then high injection speeds facilitate the filling of microcavities [33].

TABLE 1. Values of the best scale pertinence function $\Theta(k_m)$ and interaction one $\Theta(k_m,k_n)$.

(k_{m})	q_{opt}	d_{opt}	se	n_{opt}	L_{opt}	F_{opt}	(k_{m},k_{n})	q_{opt}	d_{opt}	se	n_{opt}	L_{opt}	F_{opt}
cp	R_a	2	PID	15	1.4	46	T*v	R_a	2	PID	93	9.2	348
cp	R_a	2	ID	276	27.5	8	T*v	R_a	2	ID	82	8.1	179
tr	R_a	2	PID	234	23.3	50	T*cp	R_a	2	PID	9970	996.9	39
tr	R_a	2	ID	428	42.7	28	T*cp	R_a	2	ID	4	0.3	27
T	R_a	2	PID	225	22.4	433	T*tr	R_a	2	PID	21714	2171.3	28
T	R_a	2	ID	243	24.2	532	T*tr	R_a	2	ID	14	1.3	11
V	R_a	2	PID	897	89.6	551	V*cp	R_a	2	PID	17	1.6	31
V	R_a	2	ID	852	85.1	562	V*cp	R_a	2	ID	261	26	106
							V*tr	R_a	2	PID	834	83.3	51
							V*tr	R_a	2	ID	31713	3171.2	27
							cp*tr	R_a	2	PID	10070	1006.9	16
							cp*tr	R_a	2	ID	11933	1193.2	70

n_{opt} represents the number of sampling points in the evaluation length L_{opt} for the roughness measured perpendicular to the flow (PID) and roughness measured in the flow direction (ID).

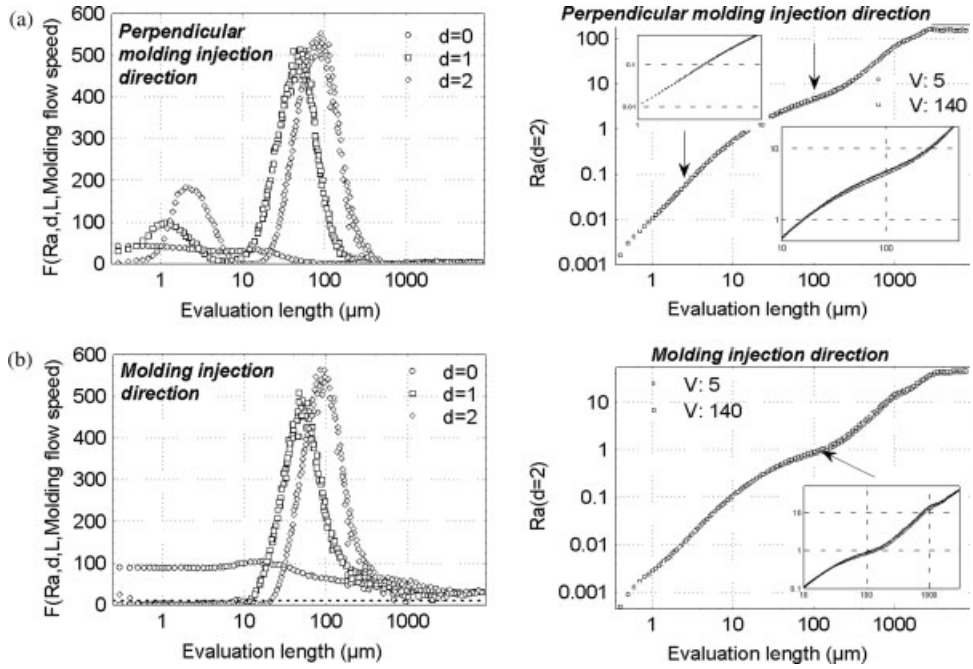

FIG. 7. Evolution of the scale pertinence functions $F\left[R_a(d_j, L, v)\right]$ versus evaluation length L due to the effect of the flow speed ($v = 5$ and 140 mm/s) calculated from a reference line of $d_j = \{0, 1, 2\}$ degree polynomial equation and the evolution of the mean Ra parameters (reference line is a two degree polynomial equation) versus the scanning length. (a) Roughness measured perpendicular to the flow and (b) roughness measured in the flow direction.

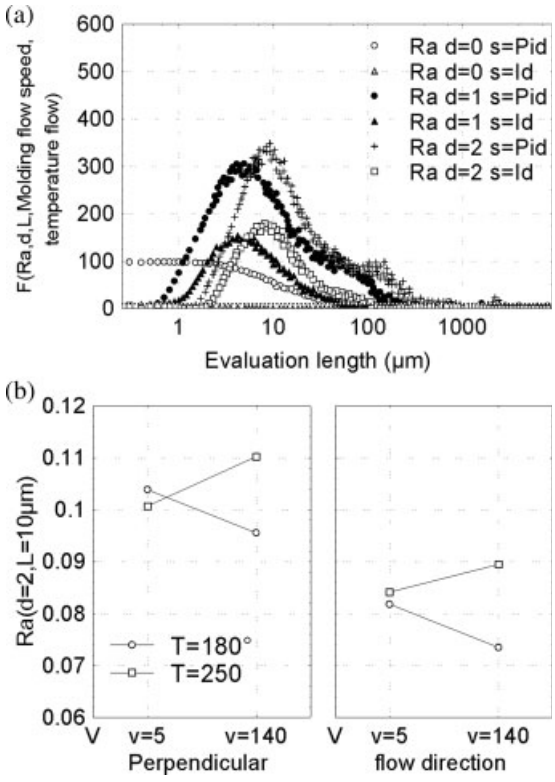

FIG. 8. (a) Evolution of the scale pertinence functions $F\left[R_a(d_j, L, T, v)\right]$ versus evaluation length L due to the effect of interaction between flow speed and temperature calculated from a reference line of $d_j = \{0, 1, 2\}$ degree polynomial equation for the two direction flows. (b) Value of the R_a at the most pertinent scale for the interaction configuration of the flow corresponding to both directions.

The Influence of the Interaction Between Temperature and Molding Injection Velocity. The correlation between temperature and injection velocity is very important and cannot be absolutely rejected [$\Theta(T, V)_{\mathrm{PID}} = (349, R_a, 2, 9)$ and $\Theta(T, V)_{\mathrm{ID}} = (179, R_a, 2, 8)$ Fig. 8a]. It can be noticed that the scale of interaction effects lays around 10 μm, a scale on which we have proved that the velocity has no effect. This clearly means that another physical effect occurs during the molding process. The interaction effect does not depend on the flow direction. At lower injection speed, there is no effect of temperature (Fig. 8b). On the contrary, at higher injection speeds, roughness increases with temperature. This interaction can be explained as follows: at low injection speed, time is enough to fill in the microroughness (10 μm of evaluation scale) and consequently, a low effect of temperature is observed. Conversely, for high injection speed, time is not sufficient to fill in the microroughness at low temperature (high viscosity) and then high temperature (low viscosity) is required to fill it in [34].

The same analysis is processed on other process parameters with their associated interactions, and it appears that their effect is lower than those described previously (see Fig. 9).

CONCLUSION

We have presented an original generic method that allows finding the evaluation length on which classical parameters must be estimated. Thanks to an experimental

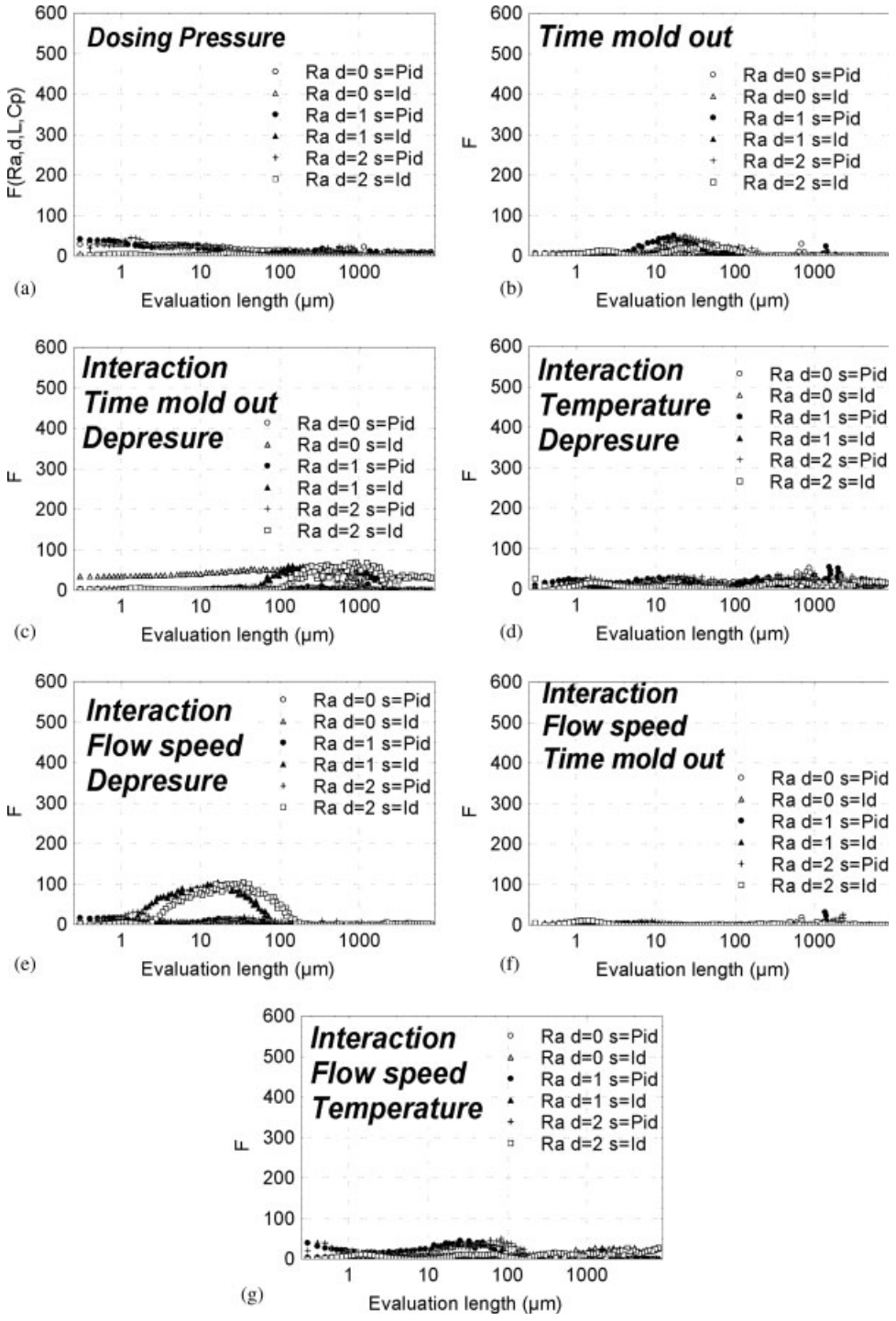

FIG. 9. Evolution of the scale pertinence function $F\left[R_a(d,L,k_j)\right]$ and $F\left[R_a(d,L,k_j,k_{j'})\right]$ for less influent process parameters.

design, it was shown that this length depends on the molding process itself. Therefore, it seems irrelevant to compare roughness parameters evaluated at a unique scale to quantify different process effects on the surface morphology. It was emphasized that no roughness parameters are relevant for all process parameters at the full scanning length, which leads to conclude erroneously that all process parameters do not affect roughness. By our multi-scale analysis coupled with an efficient statistical protocol, it was shown that the three well-known amplitude roughness parameters, R_a, R_t, and R_q get the same power of discrimination at the same scale, which leads to redundancy, providing no more information on the surface properties.

Other roughness parameters will be included further in our analytical system to try to characterize better surfaces

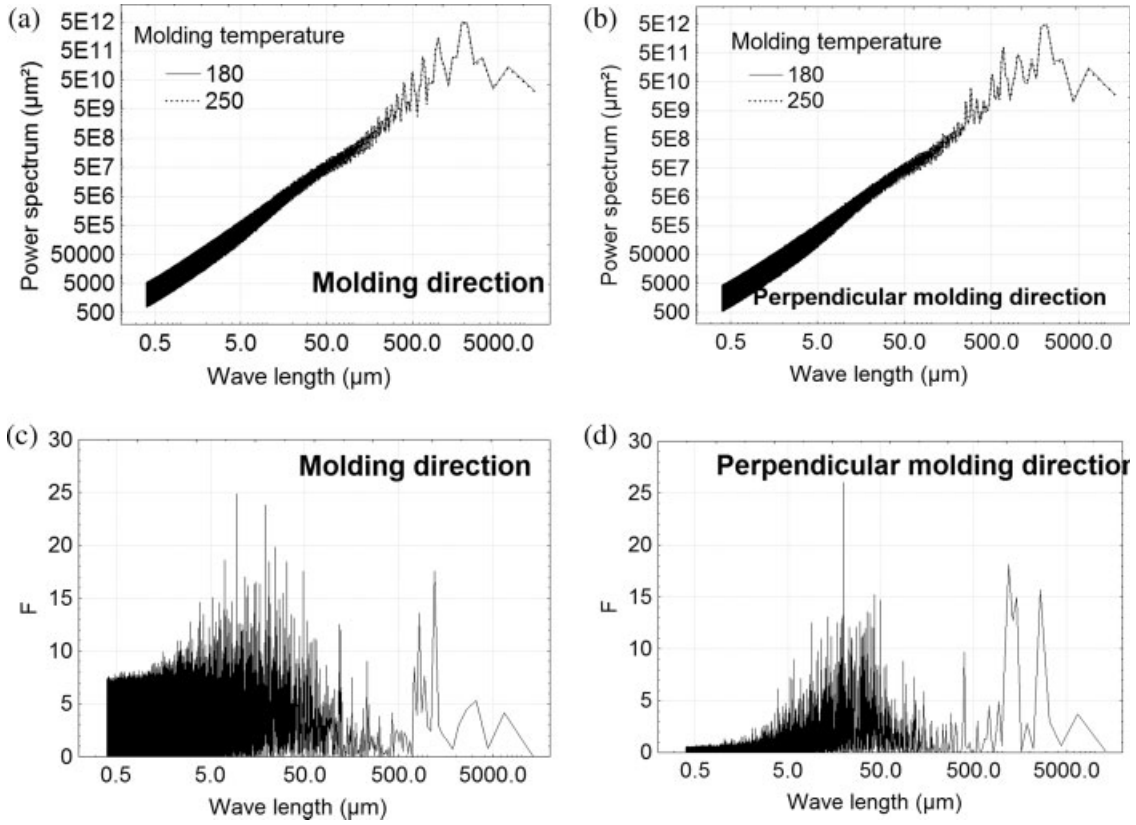

FIG. 10. Evolution of the mean power spectrum R_a parameter versus the wave length for two injection temperatures (180 and 250°C). (a) Roughness measured in the flow direction and (b) roughness measured perpendicular to the flow. Figure (c) and (d) represents the evolution of the scale pertinence function F of the spectrum versus the wave length due to the effect of the temperature injection $k_m = T$.

at different scales. Another improvement is to give confidence intervals to the multiscale discriminating function by using bootstrap protocols. Other engineering surfaces are under study by this method, and results are in good agreement with our expectations. Thanks to the use of the generalized linear model, both qualitative and quantitative process parameters can be analyzed by the proposed methodology.

ACKNOWLEDGMENTS

Authors thank Jean-Yves Delattre, Alain Demoulin, Franck Drumez from Visteon Company located at Harnes (France) for their technical assistance, Michèle Guigon for pertinent advice, and Véronique Hague for her assistance in English.

APPENDIX: COMPARISON WITH OTHER METHODS: CLASSICAL ONE AND FOURIER ANALYSIS

It could be obvious to compare the efficiency of the multiscale approach with the usual method used in the context of surface measurements. This comparison was made by Jordan and Brown [35] by differentiating measurements of polyethylene ski bases (i.e., sliding interfaces) that were stone-ground under different conditions. They show that the relative area as determined by area-scale fractal analysis is the most consistent parameter for differentiating the ground polyethylene surfaces, better than FFT or the conventional parameters used in this study. The conventional parameters correspond to the parameters when the evaluation length is equal to the scanning length meaning that roughness parameters are computed on the whole scale. By analyzing all values on the F graphs (Figs. 5–9), it is visually observed that roughness parameters are not relevant on the whole scale.

Fourier analysis is the decomposition of a signal in terms of sinusoidal functions of different frequencies that can be recombined to obtain the original signal. The roughness profile preferably measured is split up by Fourier analysis into the wave frequencies and the associated amplitudes. The Fourier coefficients can be calculated by fast Fourier transform. An amplitude mean value may be established for each wave frequency that allows computing the spectral density of the wave. A high intensity (or mean amplitude) in one of the band always corresponds to a certain physical appearance of the surface at this given scale. Figure 10a and b represents the mean power spectrum for two-injection directions and two-injection

temperatures. At high wave lengths, a peak appears at $L = 2200\ \mu m$ that corresponds to the period of the motif (Fig. 2a). Then the harmonics are found on a large band of the spectrum. The decrease of these harmonic amplitudes is low due to the fact that the shape of the periodic motif leads to a low convergence of the spectrum. These harmonics introduce a large noise at low wavelength, and so it becomes difficult to distinguish the temperature effect from the microroughness. To compare this multiscale analysis with our method, the same methodology described in this article will be applied. The F is computed on the experimental design, but rather taking into account the value of the roughness parameters at the given evaluation length, the amplitude of the spectrum is taken at each wave frequency. Then, both methods can be compared by their F values. Figure 10c and d, which represent the multiscale F versus the wave length, shows high noise amplitude. Compared to Figs. 5a and b, the maximal F value that is around 30 times lower meaning than the Fourier method is not relevant to distinguish the temperature effect on the microroughness. All the injection parameters are tested and confirmed our analysis: the F curves are all noisy, and no scale of relevance was clearly found. A Fourier analysis can be used to characterize the structural morphology induced by the process except for the macroscopic periodical motif.

REFERENCES

1. C.A. Griffiths, S.S. Dimov, E.B. Brousseau, and R.T. Hoyle, *J. Mat. Proc. Tech.*, **189**, 418 (2007).
2. N. Balabanava, R. Wierzbicki, M. Zielecka, and Z. Rymuza, *Microelectron. Eng.*, **84**, 1227 (2007).
3. V. Janarthanan, P.D. Garett, R.S. Stein, and M. Srinivasarao, *Polymer*, **38(1)**, 105 (1997).
4. D.S. Rosa, N.T. Lotto, D.R. Lopes, and C.G.F. Guedes, *Polym. Test*, **23**, 3 (2004).
5. H. Ochs, J. Vogelsang, and G. Meyer, *Prog. Org. Coat.*, **46**, 182 (2003).
6. N.R. Washburn, K.M. Yamada, C.G. Simon, S.B. Kennedy, and E.J. Amis, *Biomaterials*, **25**, 1215 (2004).
7. T. Sasaki, N. Koga, K. Shirai, Y. Kobayashi, and A. Toyoshima, *Precision Eng.*, **24**, 270 (2000).
8. P.A. Dearnley, *Wear*, **225–229**, 1109 (1999).
9. M. Motomatsu, T. Takahashi, H. Nie, W. Mizutani, and H. Tokumoto, *Polymer*, **38(1)**, 177 (1997).
10. S.W. Wai, G.M. Spinks, H.R. Brown, and M. Swain, *Polym. Test*, **23**, 501 (2004).
11. A. Larena, F. Millan, G. Perez, and G. Pinto, *Appl. Surf. Sci.*, **187**, 339 (2002).
12. K.Q. Xiao and L.C. Zhang, *Int. J. Mech. Sci.*, **44**, 2317 (2002).
13. N.S. Eis and J. Hanchi, *Tribology Int.*, **31(11)**, 653 (1998).
14. T.R. Thomas, *Rough Surfaces*, *2nd ed.*, Imperial College Press, London (1999).
15. M. Bigerelle, D. Najjar, and A. Iost, *J. Mater. Sci.*, **38(11)**, 2525 (2003).
16. C.A. Brown and S. Siegmann, *Int. J. Mach. Tools Manuf.*, **41(13–14)**, 1927 (2001).
17. R.S. Scott, P.S. Ungar, T.S. Bergstrom, C.A. Brown, F.E. Grine, M.F. Teaford, and A. Walker, *J. Hum. Evol.*, **51**, 339 (2006).
18. R.S. Scott, P.S. Ungar, T.S. Bergstrom, C.A. Brown, F.E. Grine, M.F. Teaford, and A. Walker, *Nature*, **436**, 693 (2005).
19. P. Narayan, B.C. Hancock, R. Hamel, T.S. Bergstrom, B.E. Childs, and C.A. Brown, *Mater. Sci. Eng. A*, **430(1–2)**, 79 (2006).
20. G. Farin, *Curves and Surfaces for Computer-Aided Geometric Design—A Pratical Guide*, *4th ed.*, Academic press, New York (1996).
21. V. Niola, G. Nasti, and G. Quaremba, *J. Mater. Process. Tech.*, **164–165**, 1410 (2005).
22. A.L. Wang, C.X. Yang, and X.G. Yuan, *Tribology Int.*, **36**, 527 (2003).
23. B. Josso, D.R. Burton, and M.J. Lalor, *Comp. Methods Appl. Mech. Eng.*, **191(8–10)**, 829 (2001).
24. G. Reisel and R.B. Haimann, *Surf. Coat. Tech.*, **185**, 215 (2004).
25. A.T. Manninen, *Physica A*, **319**, 535 (2003).
26. C. Tricot, *Compos. Sci. Tech.*, **63**, 1089 (2003).
27. M. Bigerelle, D. Najjar, and A. Iost, *Wear*, **258(1–4)**, 232 (2005).
28. A.J. Dobson, *An Introduction to Generalized Linear Models*, *2nd ed.*, Chapman & Hall, London (2001).
29. A. Gelman, *Ann. Stat.*, **33(1)**, 1 (2005).
30. P. McCullagh and J.A. Nelder, *Generalized Linear Models*, *2nd ed.*, Chapman & Hall, London (1989).
31. A. Frick, C. Stern, and U. Berger, "Manufacturing of High Quality Micro Prototypes by Injection Molding Using Hybrid Mould Technology," in *Proceedings of First International Conference on Multi-Material Micro Manufacture*, W. Menz and S. Dimov, Eds., Kurstruhe, Germany, 107 (2005).
32. Y.C. Su, J. Shah, and L. Lin, *Inst. Phys. Publ. J. Micromech. Microeng.*, **14**, 422 (2004).
33. M. Yoshii and H. Kuramoto, *Polym. Eng. Sci.*, **34(15)**, 1215 (1994).
34. O. Kemmann and L. Weber, "Thin Wall Molding," in *Simulation of the Micro Injection Molding Process, Specialised Molding Techniques Book*, SPE Antec, New York, 165 (2000).
35. S.E. Jordan and C.A. Brown, *Wear*, **261(3–4)**, 398 (2006).